Tropical Gastroenterology 2021;42(1):1-13

Original Article

Imaging Insights into EHPVO Induced Portal Biliopathy and its Grading: Retrospective Study Over A Decade at A Tertiary Care Hospital

Shalini Thapar Laroia[1], Komal Yadav[1], Senthil Kumar[2], Guresh Kumar[3], Ragini Kilambi[2], Shridhar Vasantrao Sasturkar[2], Tushar Kanti Chattopadhyay[2], Shiv Kumar Sarin[4]

[1]Department of Radiology, [2]Department of HPB Surgery and Liver Transplantation, [3]Department of Research, [4]Department Hepatology, Institute of Liver and Biliary sciences, New Delhi, India.

Corresponding Author: *Dr Shalini T Laroia*
Email: thaparshalini@gmail.com

ABSTRACT

Background and Aim: There is limited data on imaging features of extra hepatic portal venous obstruction (EHPVO) induced portal biliopathy. We describe a decade long experience of imaging spectrum of EHPVO induced portal biliopathy using MR/CT in a referral centre for liver diseases.

Methods: Retrospective data of patients with primary EHPVO on contrast magnetic resonance imaging MRI/ computed tomography (CT) (n=120) and portal biliopathy (PB) on subsequent magnetic resonance cholangiopancreatography (MRCP) (n=80/120) between June 2009 - 2019 was collected. Categorisation of portal biliopathy was as per the Sarin classification and the corresponding, relevant imaging parameters were studied and analysed.

Results: Sarin Type 1 biliopathy was present in 16.3 %, Type 2 in 13.8%, Type 3a in 8.8% and Type 3b in 61.3%patients. The median total serum bilirubin was 1.6 (0.9-3.4) mg/dl with a mean CBD diameter of 6.7 ± 2.9 mm. Bilobar and unilobar IHBRD were observed in 87.5% and 6.3% patients respectively. The mean CBD angle was 138.9 ± 18.8º. CBD showed smooth wall contours (10%), extrinsic indentations (83.8%) and smooth strictures (6.3%). The median CBD stricture length was 26 mm (1.25- 45 mm). Pre-stenotic dilatation was observed in 66.3% with stricture length >16 mm (sensitivity 81.1 % specificity 78%) predisposing to it. Statistically significant associations were tabulated according to the classification of PB.

Conclusion: This study provides the decade long experience of imaging findings in EHPVO induced portal biliopathy according to its classification and its clinical implications.

KEYWORDS: Portal biliopathy; EHPVO; Grading, Sarin's classification, CT; MRI/MRCP.

Introduction

Extrahepatic portal vein obstruction (EHPVO) is the most common cause of portal hypertension in the paediatric population in the eastern part of the world and the second commonest cause of adult portal hypertension in India and western continents.[1] EHPVO, by virtue of its definition, is primary thrombosis of the extrahepatic portal vein, with or without synchronous involvement of the spleno-portal axis, superior mesenteric and splenic veins. The intrahepatic divisions of the portal vein are also involved in few cases.[2,3] Changes in the extra and intrahepatic biliary system are a result of extrinsic compression and intrinsic ischemic effects on the bile duct wall caused by extensive peri-biliary collaterals.[4] The natural course of the disease is variable but remains clinically silent for prolonged periods although changes may be evident quite early. The major advantage of imaging modalities such as ultrasound, colour Doppler, CT and MRI studies is the fact that primary diagnosis of portal vein thrombosis, the extent of the thrombosis, chronicity of thrombus, amount of luminal occlusion, spleen enlargement and presence of PB can easily be deciphered, early on in the disease. This gives the clinician a head-start, for deciding the plan of management.

The purpose of our study was to assess the spectrum of imaging findings in all patients with primary EHPVO induced portal biliopathy on regular follow up, over the last ten years.

Methods

Study settings and design: This was a retrospective study of imaging characteristics of patients with EHPVO induced portal biliopathy who presented to our tertiary liver institute between June 2009 - June 2019. It was approved by the institutional ethics committee. The study design has been depicted in an algorithm in (**Figure 1**).

Methods: Data was extracted from the imaging records of patients with EHPVO (defined on contrast-enhanced CT/ MR imaging) associated portal biliopathy (defined on MRCP study). Patients with secondary aetiology of portal vein thrombosis or biliopathy such as hepatic and pancreatic malignancies, chronic liver disease, sclerosing cholangitis and biliary calculi were excluded. Portal biliopathy was classified as per the Sarin classification.[5] Imaging parameters such as intra and extra-hepatic biliary radicle dilatation, bile duct characteristics (presence of stricture, length of stricture, pre-stenotic dilatation), biliary calculi, portosystemic and paracholedochal collaterals, liver morphology, spleen size and ascites were recorded. The initial imaging findings were correlated with liver function tests.

Imaging Technique: Dynamic triple-phase MDCT study was performed on a 64-row spectral CT scanner. Scan parameters included: 120 kV with automated mA, 0.6 s rotation time, speed 55 mm/rotation, pitch of 1.375:1, detector coverage of 40 mm, and matrix size of 512 × 512. Low osmolarity non-ionic contrast medium @1.5-2.0 ml/kg body weight with iodine concentration of 400 mg/ml was administered intravenously at a rate of 4 ml/ using bolus tracking software with the reconstruction of slices @ 2.5 mm thickness.

MRCP imaging was performed on a 3 Tesla scanner using a phased array TORSOPA coil. Imaging protocol for sequences obtained was: (a) two-dimensional fast imaging employing steady-state acquisition (2D FIESTA) sequences in axial and coronal planes with a

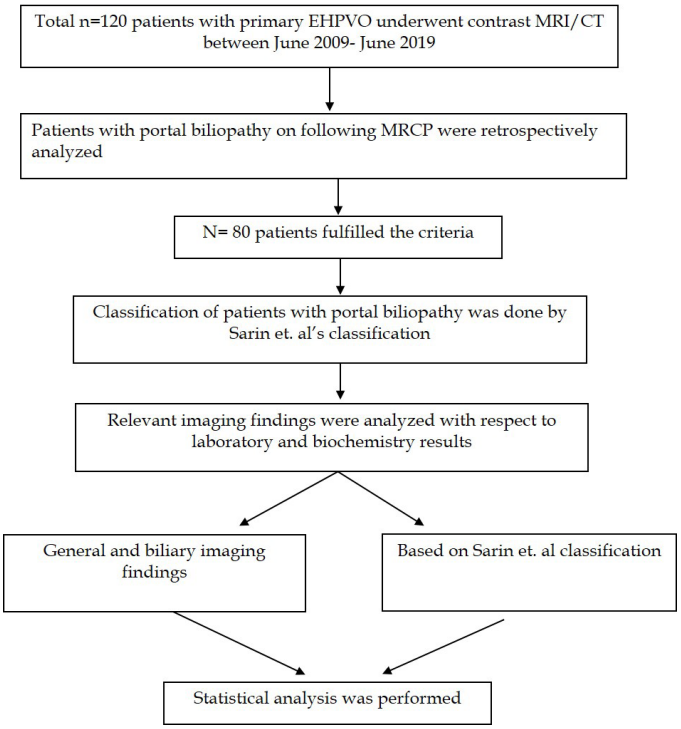

Figure 1: Study design depicting the methodology and patient selection of the study.

slice thickness of 3 mm and at 0.5 mm intervals. (TR 4.7 ms, TE 2.1 ms, slab thickness 3 mm, FOV 35 cm, flip angle 70°, and matrix 224 × 352 (b) Three-dimensional magnetic resonance cholangiopancreatography (3D MRCP) sequences were obtained (in axial and coronal planes) using respiration triggered heavily weighted T2 sequence FRFSE-XL) with contiguous thin sections (1.4 mm/0.7 overlaps). (c) T2 SSFSE sequences (with breath-hold) in thick slabs of 40 mm in coronal oblique planes at 20° increments, keeping the common bile duct as the centre of rotation. Imaging parameters for SSFSE sequences included: Repetition time (TR) 2100 ms, time to echo (TE) 80.1 ms, slab thickness 0.5 mm, field of view (FOV) 38 cm, and matrix 288 × 192. (d) Unenhanced axial sequences with a slice thickness of 5 mm at 1 mm intervals, including T1W and T2W single shot fast spin-echo (SSFSE) sequences with and without fat suppression (e) For contrast-enhanced MRI studies, Dynamic T1weighted fat-suppressed sequence was performed in addition to the above sequences using MR specific Gadolinium-based i.v contrast @1.5-2.0 ml/kg body weight administered intravenously at a rate of 4 ml/ minute using pressure injector.

Analysis of imaging: The following imaging characteristics were defined and documented for all patients.

- EHPVO was defined as non-opacified main portal vein, replaced or supplemented by multiple tortuous periportal enhancing venous collaterals (cavernoma). The extent of cavernoma was determined as intrahepatic, extra-hepatic or both (**Figure 2**)
- Liver morphology was defined as normal, chronic liver disease or cirrhotic architecture (**Figure 3a, b, d**)
- Spleen span (craniocaudal span in coronal sections with the longest measurement in cm was calculated) (**Figure 3c**)
- Presence of splenic vein and/or superior mesenteric vein thrombosis (**Figure 4**)
- The presence of paracholedochal [parallel to common bile duct (CBD)] and epicholedochal (on the surface of CBD) venous plexus and pericholecystic collaterals was identified e.g. (**Figure 5**)
- Gall bladder (GB) calculi and varices along the wall e.g. (**Figure 6**)
- Presence of portosystemic collaterals (e.g. perigastric, paraesophageal, perisplenic, mesenteric, peri-rectal, peripancreatic) (**Figure 7**)
  - ➤ Mild to moderate IHBR dilatation was defined as < 4mm dilatation of secondary intrahepatic bile ducts (**Figure 8a-c**)
  - ➤ Severe dilatation was defined as > 4mm dilatation of secondary intrahepatic bile ducts ductal e.g. (**Figure 8d**)

These were calculated on 2D and 3D MRCP sequences using electronic callipers provided on the MRI system workstation (ADW 4.4, GE)

- CBD wall contours:
  (a) Smooth CBD contour: defined as no visible contour abnormality e.g. (**Figure 9a**)

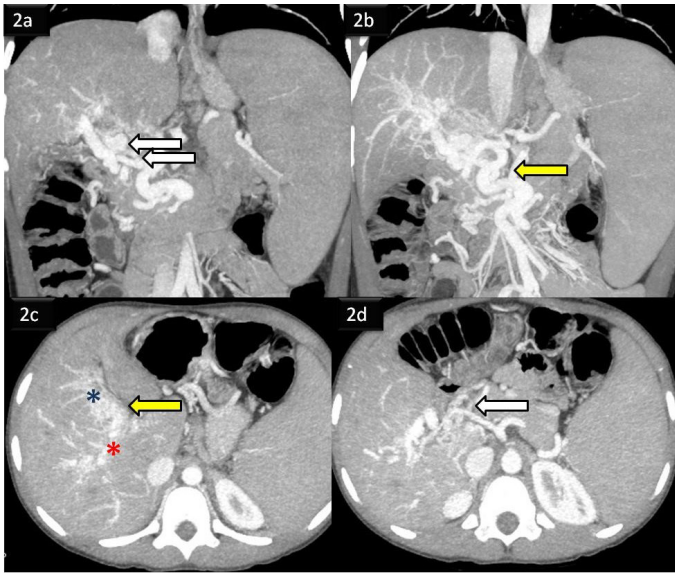

Figure 2: Dynamic CT scan of the upper abdomen with reconstruction and post-processed images depicting classical features of EHPVO with both intra and extrahepatic cavernoma; (a): Coronal Minimum intensity projection [MIP] showing the original portal vein replaced by a bunch of collaterals (white arrow) extending along with the entire spleno-portal axis; (b): (yellow arrow) Extrahepatic cavernoma; (c): Axial section of contrast CT (CECT) of the liver shows multiple collaterals replacing the intra-hepatic divisions (blue and red asterisk) of the portal vein (Intrahepatic cavernoma); (d): Axial section of the liver at porta reveals portal cavernoma with mildly dilated bile duct surrounded by paracholedochal collaterals (white arrow).

(b) Wavy or mild indentations: nodular, thumb-like or shallow impressions along the duct wall e.g. (**Figure 9b**)

- Stricture as :
  - long segment stricture (> 2cms) (**Figure 9c**)
  - short segment stricture (< 2cms) (**Figure 9d**)
- Type of Biliopathy: further graded as per Sarin *et al*. classification: On the MRCP images (using both 2D and 3D sequences)
  (a) Type 1 was defined as involvement of extrahepatic bile duct only (**Figure 10a, b**)
  (b) Type 2 was defined as involvement of intrahepatic bile ducts only (**Figure 10c**)
  (c) Type 3a was defined as involvement of extrahepatic bile duct and unilateral intrahepatic bile duct (left or right) (**Figure 10d**)
  (d) Type 3b was defined as involvement of extrahepatic bile duct and bilateral intrahepatic ducts (**Figure10e**)
- Common bile duct angle: Bile duct angle was measured in each patient by measuring the intersection of lines drawn along the long axis of the common bile duct. (**Figure 11**)

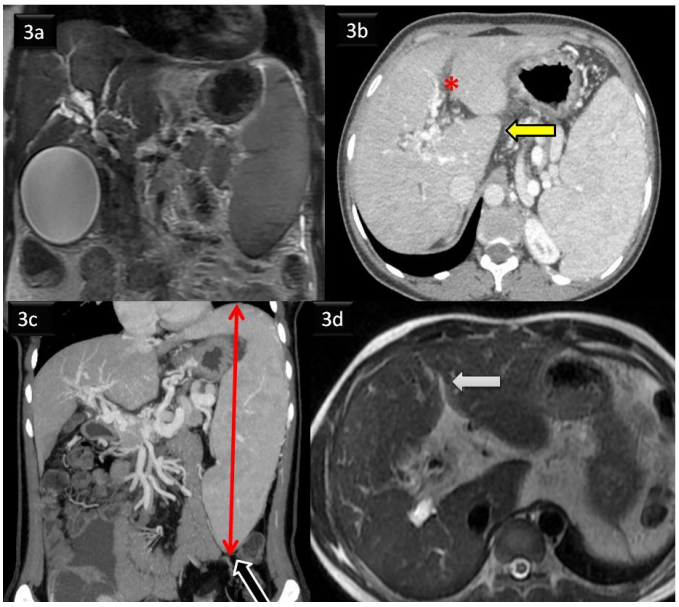

Figure 3: Dynamic CT scan of the upper abdomen showing liver and spleen morphology in patients with primary EHPVO and biliopathy. (a): Normal liver morphology with portal cavernoma and biliopathy; (b): Caudate lobe hypertrophy (arrow) with widened periportal and interlobar fissure space (*) suggestive of chronic liver parenchymal disease; (c): Massive splenomegaly with craniocaudal span (red arrow) as measured, extending to the left iliac fossa in a patient with EHPVO; (d): Cirrhosis liver with EHPVO and portal biliopathy: nodularity and irregular surface of the liver with widened periportal space.

Figure 4: Contrast-enhanced CT of the spleno portal axis in the portal venous phase in a patient with primary EHPVO and early biliopathy. (a): Collateral formation along the course of thrombosed retropancreatic splenic vein (white arrow); (b): Coronal section of the CT scan showing collateral formation in the location of thrombosed superior mesenteric vein (SMV) (bold black arrow).

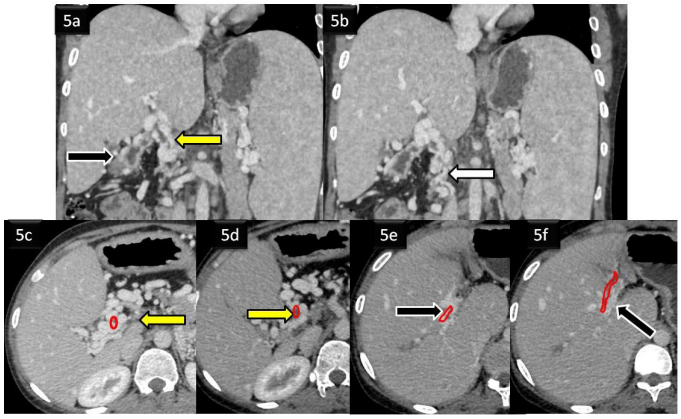

Figure 5: (a,b): Axial sections and coronal reconstruction of dynamic upper abdomen CT showing multiple tortuous collaterals in the paracholedochal location (bold yellow arrow 5a and white arrow 5b). Pericholecystic collaterals (bold black arrow 5a); (c,d): axial sections of the dynamic upper abdomen CT scan showing epicholedochal collaterals (yellow bold arrow) with central duct (red outline) in the extra-hepatic location; (e,f): axial sections of the dynamic upper abdomen CT scan showing epicholedochal collaterals (black and white arrows) with central duct (red ovoid-linear outline) in the intra-hepatic location of the left and right ductal systems.

Laboratory Parameters: Total bilirubin, Serum alkaline phosphate (SAP) and gamma-glutamyl transferase (GGT) levels were recorded to assess liver function.

Statistical Analysis

Categorical data was described as frequency and proportion. Continuous data was presented as mean with standard deviation or median with interquartile range. The comparison of means was done using student t-test or Mann Whitney U test as required.

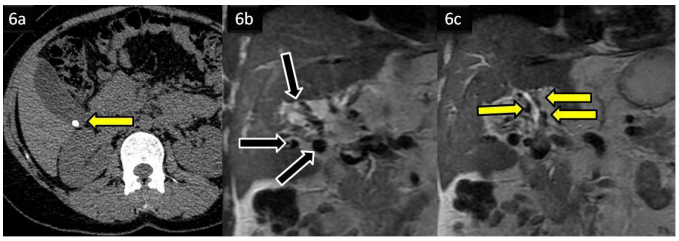

Figure 6: (a): Axial non-contrast CT in a 25-year-old lady with EHPVO showing intraluminal gall bladder hyperdense calculus (bold yellow arrow); (b,c): coronal T2WI sequence acquired on a 3T MRI scanner of a 25-year-old lady with EHPVO showing hypointense serpiginous flow voids of peri-cholecystic collaterals (bold black and white arrow) and hypointense serpiginous flow voids of paracholedochal collaterals causing smooth extrinsic impression on the duct wall (yellow bold arrows).

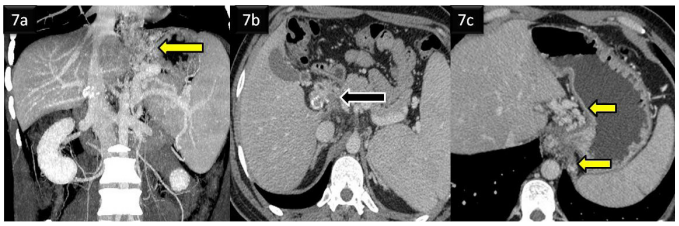

Figure 7: Dynamic CT scan of a patient (in portal venous phase) with EHPVO demonstrating various types of portosystemic collaterals; (a): Coronal MIP reconstruction of dynamic CT scan in a 30-year-old male patient with EHPVO showing gastro-oesophageal shunt pathway (yellow bold arrow); (b): Axial dynamic CT scan showing thrombosed spleno-portal axis (bold black arrow) with areas of calcification in the portal vein wall in the above patient; consistent with a diagnosis of EHPVO. (c): Axial sections of the CT scan in the patient with EHPVO showing para oesophagal collaterals (bold yellow arrow) and perigastric collaterals (bold yellow arrow).

Results

A total number of 80 patients underwent CEMRI/CECT followed by MRCP for evaluation of primary EHPVO associated portal biliopathy at our institute over ten years. The majority of the patients were men and of a young age (range 4-55 years). Intrahepatic with associated extrahepatic (combined/ complete) cavernoma formation was seen in a majority of the patients, n= 53/80 (66.2%). General characteristics of the patient population including liver morphology, types and sites of portosystemic and localized collaterals, biochemical markers, ascites, spleen size have been described in **Table 1**.

Portal biliopathy was documented in all patients in the study group and a detailed assessment of the biliary tree was performed. The imaging characteristics of the study population pertaining to the biliary system (classification, biliary dilatation, calculi, bile duct contour, and strictures) have been enumerated in **Table 2**.

CBD walls showed smooth contours (with well-visualized lumen) in 10% of patients and wavy outlines with indentation due to extrinsic periductal collateral

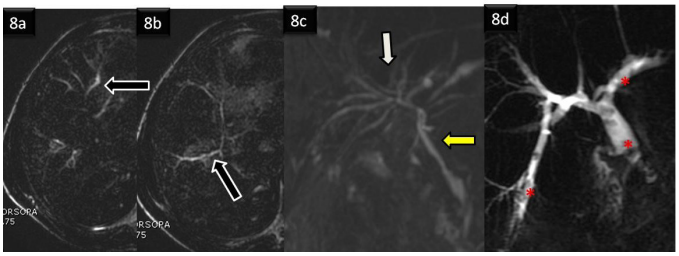

Figure 8: 2D and 3D MRCP projections for analysis of the bile duct dilatation in three different patients with EHPVO and biliopathy; (a,b): Axial 3D MRCP sequence showing mild intrahepatic bile duct dilatation involving only the right lobe (white bold outline arrows); (c): 2D MRCP sequence in a 32-year-old male patient showing extrahepatic bile duct with wavy contours (bold yellow arrow) and mild-moderate bilobar IHBRD (bold white arrow); (d): 2 D MRCP projection in a 26-year-old female patient showing intraductal filling defects (calculi) in the severely dilated extra and bilobar intrahepatic segments (*).

channels in 83.8% of patients. (**Figure 12**) The wavy thumb-printing like indentations were seen to occur due to extrinsic duct compression by tortuous collaterals in paracholedochal as well as epicholedochal locations

In 5/80 (6.3%) patients, the common duct wall was smooth with associated tight stricture of the lumen (**Figure 13**).

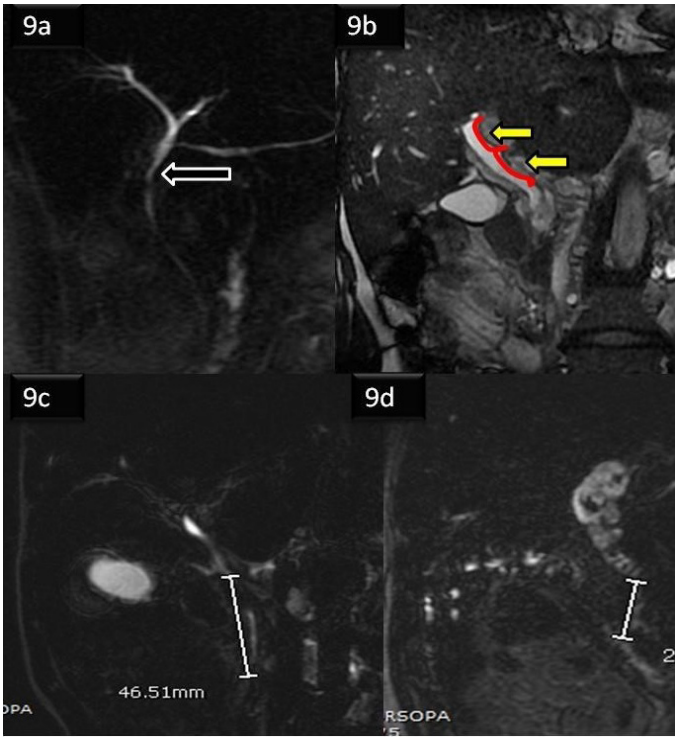

Figure 9: 2D and 3D MRCP projections for analysis and categorization of the bile duct contour and stricture in four different patients with EHPVO and biliopathy; (a): 2D MRCP sequence shows no significant or visible contour abnormality of the extrahepatic bile duct labelled as smooth contours (outlined white arrow) with mild intrahepatic bile duct dilatation; (b): Coronal FIESTA, T1WI sequence acquired on a 3T MRI scanner of a 25-year-old lady showing mildly hypointense epicholedochal collaterals along the surface of the CBD causing irregular, thumb printing like contour (red outlines) of the duct wall (bold yellow arrows); (c): 3D MRCP shows long segment extrahepatic common duct stricture with a measured length of 4cm labelled as 'long stricture (defined as length >2cm)'; (d): 3D MRCP sequence shows a grossly dilated extrahepatic duct with multiple intraductal calculi showing a small segment stricture (< 2cm), labelled as 'short stricture'

MRCP demonstrated concomitant intra and extrahepatic strictures in 17/80 (21.2%) patients. Of these, long-segment strictures (measuring > 20mm in length) were seen in 52.5% of patients and short segment strictures in 33.8% of patients.

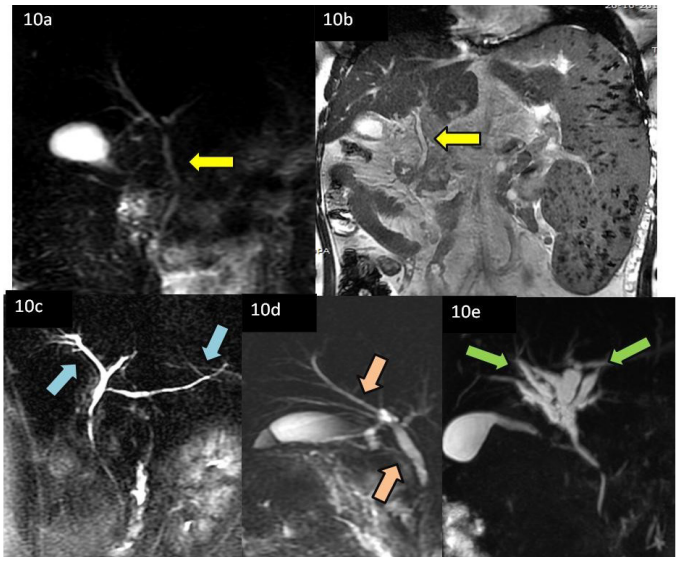

Figure 10: 2D and 3D MRCP projections of four different patients showing analysis and categorization of biliopathy as per Sarin et. al classification; (a,b): 3D MRCP and Coronal FIESTA sequence respectively, show Type 1 biliopathy defined as involvement of extrahepatic bile duct (bold yellow arrows); (c): Type 2 biliopathy was defined as involvement of intrahepatic bile ducts only (bold blue arrows); (d): Type 3a was defined as involvement of extrahepatic bile duct and unilateral intrahepatic bile duct (left or right) (bold orange arrows); (e): Type 3b was defined as involvement of extrahepatic bile duct and bilateral intrahepatic ducts (bold green arrows).

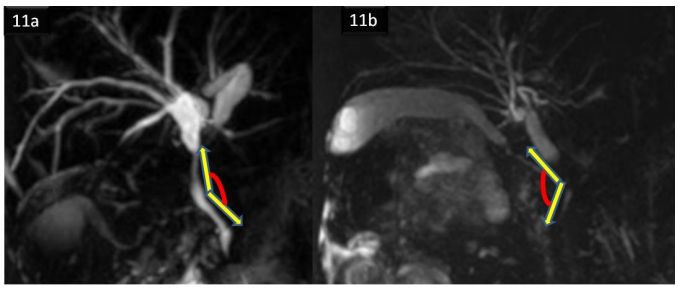

Figure 11. Calculation of CBD angulation along its axis on 3D MRCP projections; (a): The angle of CBD > 145º (red arc); (b): 3D MRCP projection in a 32 year old male patient with CBD angulations along its axis of < 145º (red arc).

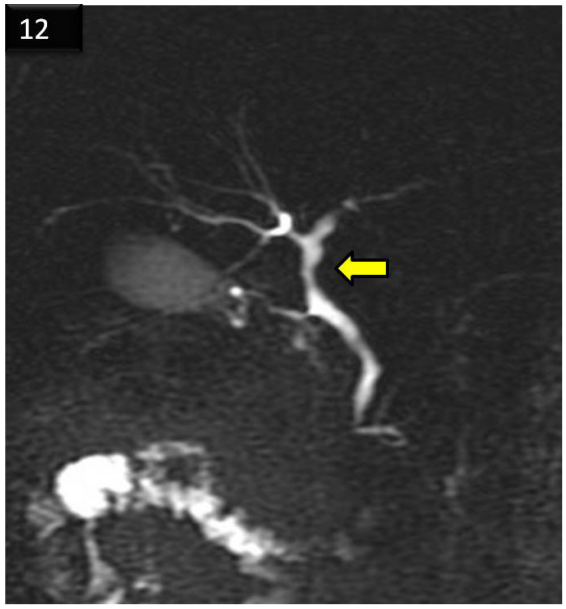

Figure 12: 3D coronal MRCP projection of a 46-year-old male patient with Type 3a portal biliopathy showing mildly dilated, irregular contoured CBD (yellow arrow) with thumb printing due to tortuous collaterals, without intraductal filling defects-calculi. Patient was treated with conservative and medical management.

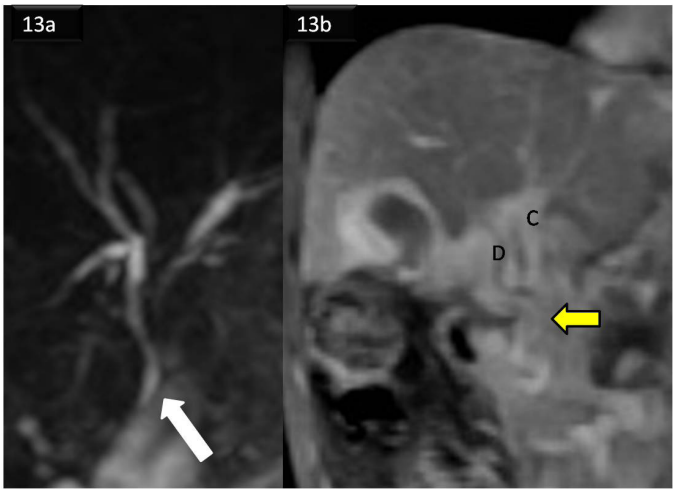

Figure 13: (a): 2D MRCP projection of a 17-year-old young boy showing smooth, (without any contour abnormality) long, tight stricture of the mid and lower end of the CBD (bold white arrow) with mild upstream biliary prominence; (b): Contrast enhanced coronal sections of T1WI of dynamic MR examination of the same patient shows multiple collaterals; (c): along the common hepatic duct d. with narrowing of the duct beyond the middle segment (bold yellow arrow).

Stricture length of >16 mm (sensitivity 81.1 % and specificity 78%, AUC= 89.2) was found to be a predisposing factor for pre-stenotic dilatation. (**Figure 14**)

Imaging characteristics, laboratory parameters and general factors were further compared amongst the four groups (type 1-3a and 3b) of portal biliopathy according to Sarin classification. These are enumerated in **Tables 3** and **4**. The statistically significant predictors were: CBD, RHD and LHD diameters', presence of gall

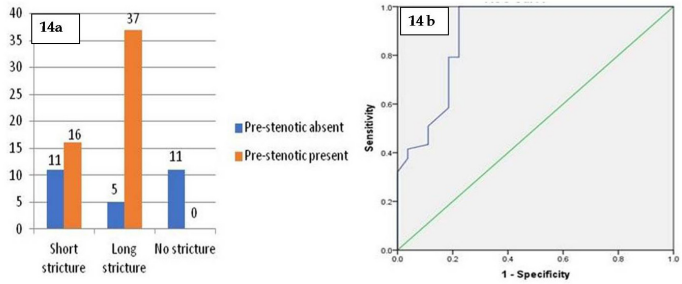

Figure 14: (a): Bar graph depicting pre-stenotic dilatation, seen proximal to the stricture, amongst patients; (b): Stricture length of ≥16 mm (AUC= 89.2) was found to be a predisposing factor for pre-stenotic dilatation.

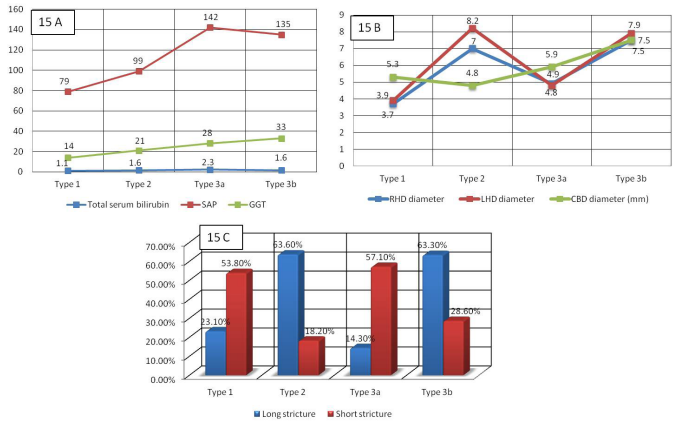

Figure 15: (a): Comparison of different groups of Portal Biliopathy with liver function parameters (serum bilirubin, SAP and GGT); (b): Comparison of the four groups with RHF, LHD and CBD; (c): Distribution of long and short strictures amongst the sub-classified groups of portal biliopathy.

bladder sludge, smooth CBD contour, unilobar IHBRD, presence of intrahepatic duct stricture, length of stricture and short segment stricture (measuring <20mm). Pre-stenotic dilatation was also statistically significant amongst the classified groups.

Discussion

Most of the studies in the literature have illustrated results of EHPVO and its impact on the biliary system (biliopathy) with the help of endoscopic retrograde cholangiography (ERC).[4] Our study has, for the first time, analyzed the evolution of PB on CT and MRCP with clinical and laboratory corroboration. We have secondarily compared of various imaging parameters amongst the sub-classes of PB and identified significant markers on MRCP. To the best of our knowledge, no previous study has been performed with the above components over a decade's timeline.

Our study population revealed a young demographic predisposition (mean age: 24.8 ± 11.5 years, range 4-55 years) to develop PB after primary EHPVO. This suggests an early onset of cholangiopathy with pre-existing primary disease. Our results show a younger mean age of development of biliopathy compared to other studies.[6,7] There is probably a population of young adults in the early second decade and possible late adolescence with long term asymptomatic or undiagnosed EHPVO who present much later with symptoms of biliopathy either clinically or through abnormal liver function tests. 8 Non-invasive investigations such as MRCP or CT, which are easily available at the secondary and tertiary healthcare setting, would be useful to detect early changes of PB in these patients to optimize the timeframe for adequate management. Young patients suffering from the silent and asymptomatic stage of EHPVO with PB would benefit from intensive screening with ultrasound or MRI for the primary diagnosis and close clinical surveillance after the diagnosis.

Table 1: General characteristics of the patient population.

General Characteristics		Frequency
Age (mean ± std.)		24.8 ± 11.4
Gender M/F		58/22
Liver Morphology	Normal	14 (17.5%)
	Cirrhotic	25 (31.2%)
	Chronic liver disease	41 (51.2%)
Total bilirubin (mm) (median IQR)		1.6 (0.9-3.4)
SAP median (IQR)		127 (75.2 -210.7)
GGT median (IQR)		25.5 (14 - 76.7)
Exclusive intrahepatic cavernoma, n (%)		6 (7.5%)
Exclusive extrahepatic cavernoma, n (%)		21 (26.2%)
Both (intrahepatic+ extrahepatic cavernoma)		53 (66.2%)
Collaterals	Portosystemic	67 (83.7%)
	GB varices	55 (68.7%)
	EVP	59 (73.7%)
	PVP	76 (95%)
SVT, n (%)		40 (50)
SMVT, n (%)		53 (66.3)
Spleen span (mean ± s.td)		17.5 ± 4.4
Ascites, n (%)		8 (10)

SAP: Serum alkaline phosphatase, GGT: Gamma-glutamyl-transferase, GB: Gall bladder, EVP: Epicholedochal venous plexus, PVP: Paracholedochal venous plexus, SVT: Splenic vein thrombosis, SMVT: Superior mesenteric venous thrombosis.

All patients in our study group had portal cavernoma formation with PB (inclusion criteria). Development of periportal collaterals after thrombosis of the main portal vein and its divisions serves as an alternate lifeline for the hepatic portal circulation. These collateral channels surround the walls of the extrahepatic bile duct and its intrahepatic divisions in the paracholedochal and epicholedochal locations with subsequent bulging of the walls causing contour abnormality. Prolonged duct wall changes lead to ischemia, fibrosis and subsequent stricture formation.[9] We observed portosystemic, EVP, PVP, and GB wall collaterals in all our patients. Combined intra and extrahepatic cavernoma formation was found in a majority of the patients (66%). Sarin Type 3b group had the maximum number of patients with both intrahepatic (76%) and extrahepatic (92%) cavernoma formation amongst all groups (p=0.35, 0.74 respectively). This was probably the reason why these patients developed both bilobar intrahepatic and extrahepatic bile duct changes. This observation demonstrates the direct effect of cavernoma extent and the resultant bile duct changes.

We studied the impact of PB on liver morphology. It was observed that the majority of the patients (51%) had features of chronic liver disease (CLD) (widened periportal space, lobulated liver outlines, prominent caudate lobe and hypertrophied left lobe as compensatory changes to compromised hepatic function). Overt cirrhosis (nodular parenchyma with frank regenerative nodular areas, shrunken liver and dilated portal vein with other stigmata of portal hypertension, splenomegaly, ascites and portosystemic shunts/collaterals) was noted in (31%) patients. This feature is usually seen in the

Table 2: Imaging characteristics of the study population pertaining to the biliary system.

Biliary characteristics (n=80)		Frequency (%)
Biliopathy Classification	Type 1	13 (16.3%)
	Type 2	11 (13.8%)
	Type 3a	7 (8.8%)
	Type 3b	49 (61.3%)
IHBRD	Unilobar	5 (6.2%)
	Bilobar (mild-moderate)	28 (35%)
	Bilobar severe	42 (52.5%)
Calculi	GB calculi	22 (27.5%)
	CBD calculi	16 (20%)
CBD contour	Smooth	8 (10%)
	Wavy/indentations	67 (83.7)
	Strictured lumen	5 (6.2%)
Stricture	Intrahepatic	22 (27.5%)
	Extrahepatic	41 (51.2%)
Stricture length	Long	42 (52.5%)
	Short	27 (33.8%)
Pre-stenotic dilatation		53 (66.2%)
LHD diameter (mm) (mean ±std.)		7.1 ± 4.3
RHD diameter (mm) (mean ± std.)		6.6 ± 3.8
Stricture length median (IQR)		26 (1.25-45) 26.6±22
CBD diameter (mean ± s.td)		6.7± 2.9
CBD angle (mean ± Std)		139 ± 18.8

IHBRD: Intrahepatic biliary radical, CBD: Common bile duct, GB: Gall bladder, LHD: Left hepatic duct, RHD: Right hepatic duct.

later stages of the disease with progression to secondary biliary cirrhosis and resultant portal hypertension. Patients with decompensated cirrhosis would require active intervention for raised portal pressure in the form of portosystemic shunt surgery and hence need to be identified with the help of imaging for early management strategy. Patients with 'normal liver morphology' would be kept under surveillance with follow up MRCP or ultrasonography for early detection or rapid progression of PB during the disease course. The majority of the 'normal liver morphology' were seen in the Type 2 group, 'CLD' in Type 1 and 'cirrhotic' in Type 3a (**Table 3**). It has been understood that reduced portal perfusion causes changes in liver morphology.[10] However, the interesting observation in our study was the development of PB in patients with intact liver morphology (seen in all categories except type 3a) (**Table 3**).

The commonest type of PB seen in our group was Type 3b followed by Type 1. Similar findings were observed by Ozkavukcu *et al*., however, we further subclassified it to the Type 3b category.[11] They also reported the commonest site of stricture as the extrahepatic duct. We found extrahepatic and intrahepatic duct strictures in all subgroups, however, the highest involvement was noted in type 3a-3b, followed by type 2 and 1 respectively. (**Table 3**)

We also noted maximum intrahepatic strictures in type 2 followed by type 3a and 3b (p=0.006)

Khuroo *et al*. graded the biliary dilatation and its severity in a previous study from mild to severe by subjective assessment of the luminal narrowing as compared to normal calibre within the same duct.[12] This stratification appears to be variable from one reader to another and also depends on adequate opacification of the ductal system on cholangiography projections. It is also difficult to gauge the normal lumen on ERC, where the extra and periductal collaterals cannot be truly assessed. The severity of biliary dilatation was classified by Llop *et al*. as grade 1-3 with increasing severity and stenosis.[13]

We categorized our patients into 'types of biliopathy' as per Sarin *et al*. classification; (Table 3) As expected, severe dilatation was present in ascending order from type 1<3a<2<3b (p=0.28) whereas mild-moderate dilatation was seen in type 3a and type 1 followed by type 3b and type 2. In type 1 variety, the extrahepatic duct involvement itself seemed to cause upstream IHBRD. This is contrary to the expectation that isolated extrahepatic duct involvement would be asymptomatic.

The clinical assessment of patients suffering from primary EHPVO is usually made using laboratory parameters such as total bilirubin, SAP and GGT to estimate the ongoing hepatic damage in a functional manner. MRCP and CT imaging can be used for the subjective analysis of these parameters in a sensitive and specific manner. In our patient population, we observed that the median SAP was mildly elevated and GGT remained well within the desired range of normal values. Except for borderline total serum bilirubin levels in Type 3a, no category showed elevated bilirubin or abnormal LFT values. (**Figure 15**) These findings reinforce the importance of regular follow up imaging as a surveillance tool for these patients.

Walser *et al*. proposed that an acute angulation (median—110°) of the CBD was seen in patients with portal biliopathy14. An acute (<145°) angulation has been observed by Keizman *et al*. to predispose patients to a greater risk for intraductal calculi.[15] The study by Keizman *et al*. is based on ERC findings where an angle of 145° was considered abnormal.[4,15,16] Bhatia has reviewed various groups and their interpretation of these findings on ERC and has stressed the need for uniform criteria for the classification of these duct wall abnormalities with a special emphasis on duct angle. 4 We found that CBD angle (obtained along its axis, formed by the common duct due to pericholedochal and epicholedochal collaterals) was acute (i.e. <145°) (mean =139 ± 18.8°, range 95°-168°) in all patients but was not significant amongst various subgroups as per their classification. (**Figure 11**)

Various imaging parameters, such as, type of biliopathy (as per various classifications), biliary dilatation: gall bladder calculi, common bile duct contour abnormalities and stricture formation have been recorded as part of the spectrum of the natural course of the disease in previous studies.[13,7,17] In our study, we not only studied all of the above parameters as predictors but also included a wider range of criteria using MRCP/CT imaging such as extent and severity of biliary dilatation.

Table 3: Correlation of Imaging Parameters with Sarin type Portal biliopathy classification.

Imaging Parameters		Sarin type classification				p value
		Type 1 (n=13)	Type 2 (n=11)	Type 3a (n=7)	Type 3b (n=49)	
Age		24.6 ± 14.1	25.8 ± 11.4	20.7±11.7	25.1±10.8	0.8
Gender M/F		11/2	8/3	6/1	33/16	0.52
Total serum bilirubin		1.1 (0.6- 1.7)	1.6 (0.9- 2.1)	2.3 (1.6- 2.4)	1.6 (0.8- 5.9)	0.37
SAP		79 (62- 168.5)	99 (61- 246)	142 (67- 170)	135 (81- 219)	0.42
GGT		14 (10.5- 31.5)	21 (15- 73)	28 (24- 33)	33 (14- 127.5)	0.07
Spleen span (cm)		15.5 ±5	16.9 ± 3.8	17.4±4.9	18.2±4.1	0.23
CBD angle		137.3 ± 21.4	143.7±20.2	147.7±13.4	137.1±18.4	0.43
Cholelithiasis		1 (7.7%)	3 (27.3%)	0	9 (18.4%)	0.36
hepaticolithiasis		0	1 (9.1%)	0	1 (2%)	0.47
choledocholithiasis+ cholelithiasis		0	0	0	1 (2%)	0.88
choledocholithiasis		0	0	0	3 (6.1%)	0.57
cholecystectomy		1 (7.7%)	1 (9.1%)	0	5 (10.2%)	0.84
Liver morphology	Normal	2 (15.4%)	4 (36.4%)	0	8 (16.3%)	0.23
	Cirrhotic	3 (23.1%)	4 (36.4%)	3 (42.9%)	15 (30.6%)	0.80
	CLD	8 (61.5%)	3 (27.3%)	4 (57.1%)	26 (53.1%)	0.35
SVT		1 (7.7%)	1 (9.1%)	0	2 (4.1%)	0.79
SMVT		4 (30.8%)	2 (18.2%)	2 (28.6%)	9 (18.4%)	0.74
SVT+ SMVT		7 (53.8%)	2 (18.2%)	4 (57.1%)	23 (46.9%)	0.25
Intrahepatic cavernoma		8 (61.5%)	6 (54.5%)	5 (71.4%)	37 (75.5%)	0.35
Extrahepatic cavernoma		12 (92.3%)	10 (90.9%)	7 (100%)	45 (91.8%)	0.74
EVP		10 (76.9%)	6 (54.5%)	7 (100%)	36 (73.5%)	0.25
PVP		13 (100%)	10 (90.9%)	7 (100%)	46 (93.9%)	0.49
GB	calculi	2 (15.4%)	2 (18.2%)	1 (14.3%)	17 (34.7%)	0.88
	varices	8 (61.5%)	6 (54.5%)	4 (57.1%)	37 (75.5%)	0.19
Ascites		2 (15.4%)	1 (9.1%)	2 (28.6%)	3 (6.1%)	0.66
Portosystemic collaterals		9 (69.2%)	10 (90.9%)	5 (71.4%)	43 (87.8%)	0.34
Bilobar IHBRD	Mild to moderate	6 (46.2%)	3 (27.3%)	4 (57.1%)	15 (30.6%)	0.26
	severe	1 (7.7%)	7 (63.6%)	1 (14.3%)	33 (67.3%)	0.28
CBD contour	Wavy/mild	12 (92.3%)	8 (72.7%)	6 (85.7%)	41 (83.7%)	0.40
	stricture	0	2 (18.2%)	0	3 (6.1%)	0.26
CBD calculi		2 (15.4%)	1 (9.1%)	0	13 (26.5%)	0.25
Extrahepatic CBD stricture		3 (23.1%)	6 (54.5%)	4 (57.1%)	28 (57.1%)	0.97
Long stricture		3 (23.1%)	7 (63.6%)	1 (14.3%)	31 (63.3%)	0.63

SAP: Serum alkaline phosphatase, GGT: Gamma-glutamyl-transferase, CLD: Chronic liver disease, EVP: Epicholedochal venous plexus, PVP: Paracholedochal venous plexus, SVT: Splenic vein thrombosis, SMVT: Superior mesenteric venous thrombosis, IHBRD: Intrahepatic biliary radical, CBD: Common bile duct, GB: Gall bladder.

Table 4: Correlation of biliary imaging parameters with Sarin type Portal biliopathy.

Significant parameters	Sarin type classification				p value
	Type 1	Type 2	Type 3a	Type 3b	
RHD diameter	3.7 ± 1.9	7±3.2	4.9±2	7.5±4	0.005
LHD diameter	3.9 ± 1.4	8.2±4.7	4.8±2.6	7.9±4.4	0.006
CBD diameter (mm)	5.3 ± 1.7	4.8± 1.4	5.9±1.2	7.5±3.3	0.007
GB sludge	5 (38.5%)	1 (9.1%)	0	5 (10.2%)	0.03
CBD smooth contour	1 (7.7%)	1 (9.1%)	1 (14.3%)	5 (10.2%)	<0.001
Unilobar IHBRD	0	1 (9.1%)	3 (42.9%)	1 (2%)	0.0003
Intrahepatic bile duct stricture	0	7 (63.6%)	2 (28.6%)	13 (26.5%)	0.006
Short stricture	7 (53.8%)	2 (18.2%)	4 (57.1%)	14 (28.6%)	<0.001
Stricture length	9.4±15.7	31.8±25.2	13.2±13.9	31.9±21	0.001
Pre-stenotic dilatation	0	8 (72.7%)	3 (42.9%)	42 (85.7%)	0.009

LHD: Left hepatic duct, RHD: Right hepatic duct, GB: Gall bladder, IHBRD: Intrahepatic biliary radical dilatation.

Sarin's classification accords the type of biliopathy by duct wall abnormality and presence of biliopathy but does not consider the amount of dilatation. We observed that the development of bilobar intrahepatic biliary dilatation (IHBRD) of any degree (mild to severe), after peribiliary collaterals and development of biliopathy was a better indicator of disease progression.

We found for the first time that RHD, LHD, CBD diameters', smooth contours of CBD, GB sludge, unilobar IHBRD, intrahepatic duct strictures, pre stenotic dilatation, stricture length and short strictures were significant parameters amongst the types of biliopathy. (**Table 4**)

RHD was most dilated in type 3b followed by type 2 PB, LHD was most dilated in type 2 followed by type 3b and CBD was most dilated in type 3b and 3a categories. (**Figure 15b**)

Smooth contours of the extrahepatic duct were noted most often in type 3a, followed by 3b and type 2. GB sludge was most often present in Type 1 patients and completely absent in type 3a.

The longest stricture length was seen in type 3b and type 2 categories. Short strictures' were most often seen in type 3a. (**Figure 15c**)

In-depth studies in a larger population are required to validate these parameters as potential predictors of the extent and progression of biliopathy as well as disease severity. We demonstrated the spectrum of imaging findings from liver morphology to detailed assessment of the biliary tract in EHPVO induced portal biliopathy over a decade.

Conclusion

We propose that, from amongst several imaging features described in the literature, only a few of the relevant parameters discussed above, may be closely monitored for decision making during the disease course.

References

1. Dilawari JB, Chawla YK. Extrahepatic portal venous obstruction. Gut. 1988; 29:554– 555.
2. Franchis R, Baveno V, Faculty. Revising consensus in portal hypertension: report of the Baveno V consensus workshop on methodology of diagnosis and therapy in portal hypertension. J Hepatol. 2010;53:762–8.
3. Garcia Pagan JC, Hernandez GM. Extrahepatic portal vein thrombosis. Semin Liver Dis. 2008; 3:282–92.
4. Bhatia V. Endoscopic retrograde cholangiography in portal cavernoma cholangiopathy - results from different studies and proposal for uniform terminology. J Clin Exp Hepatol. 2014; 4 (Suppl 1):S37-43.
5. Sarin SK, Bhatia V, Makwana U. Poratal biliopathy in extrahepatic portal venous obstruction. Indian J Gastroenterol. 1992;11(suppl 1):A82

6. Khare R, Sikora SS, Srikanth G. Extrahepatic portal venous obstruction and obstructive jaundice: approach to management. J Gastroenterol Hepatol. 2005;20:56–61.
7. Kumar M, Saraswat VA. Natural history of portal cavernoma cholangiopathy. J Clin Exp Hepatol. 2014;4 (Suppl 1):S62-6.
8. Valla D, Casadevall N, Huisse MG. Etiology of portal vein thrombosis in adults. A prospective evaluation of primary myeloproliferative disorders. Gastroenterology. 1988; 94:1063–1069.
9. Puri P. Pathogenesis of Portal Cavernoma Cholangiopathy: Is it Compression by Collaterals or Ischemic Injury to Bile Ducts During Portal Vein Thrombosis? J ClinExpHepatol. 2014;4(Suppl 1):S27-33.
10. Arora A, Sarin SK. Multimodality imaging of primary extrahepatic portal vein obstruction (EHPVO): what every radiologist should know. Br J Radiol. 2015; 88(1052):20150008.
11. Ozkavukcu E, Erden A, Erden I. Imaging features of portal biliopathy: frequency of involvement patterns with emphasis on MRCP. Eur J Radiol. 2009;71:129–134
12. Khuroo MS, Yattoo GN, Zargar SA, Javid G, Dar MY, Khan BA, *et al*. Biliary abnormalities associated with extrahepatic portal venous obstruction. Hepatology. 1993; 17(5):807-1.
13. Llop E, de Juan C, Seijo S, Garcia Criado A, Abraldes JG, Bosch J, *et al*. Portal cholangiopathy: radiological classification and natural history. Gut. 2011; 60(6):853–860.
14. Walser EM, Runyan BR, Heckman MG. Extrahepatic portal biliopathy: proposed aetiology on the basis of anatomic and clinical features. Radiology. 2011;258:146–153
15. Keizman D, Shalom MI, Konikoff FM. An angulated common bile duct predisposes to recurrent symptomatic bile duct stones after endoscopic stone extraction. Surg Endosc. 2006;20:1594–1599.
16. Warren BL. Association between cholangiographic angulation of the common bile duct and choledocholithiasis. S Afr J Surg.1987;25:13–15.
17. Dhiman R, Singh P, Behera A. Diagnosis of portal hypertensive biliopathy (PHB) in patients with extrahepatic portal venous obstruction (EHPVO): endoscopic retrograde cholangiography versus MR cholangiography. J Gastroenterol Hepatol 2006; 21: A223.